Applied Energy Symposium 2020: Low carbon cities and urban energy systems
October 10-17, 2020
Paper ID: D128

Estimation of Rooftop Solar Potential using Publicly Available Geodata and Deeping Learning

Zhixin Zhang, Teng Zhong, Min Chen*, Zixuan Zhou, Yijie Wang, Kai Zhang

School of geography, Nanjing Normal University, Nanjing 210023, China

ABSTRACT

Rooftop solar photovoltaic power generation provides a feasible solution for the sustainable development of the city. The estimation of rooftop solar potential is of great significance to the formulation of urban energy plans. Quantifying the rooftop area is the basis of estimating the rooftop solar potential, but how to extract the rooftop information quickly in large-scale is still a challenge. In this study, a scalable framework is used to estimate the rooftop solar potential based on Google Earth satellite images. This framework uses a deep learning semantic segmentation method to extract the rooftop, which provides support for estimating the solar potential of the rooftop. In order to reduce the labor cost invested in the training process of the rooftop extraction model, a training data acquisition strategy was developed based on prior knowledge of the urban and rural spatial layout and landuse. This paper takes Nanjing, China as an example to make an empirical analysis. The results show that the framework can achieve good rooftop extraction effect. It is also found that the solar potential of buildings in Nanjing is huge.

Keywords: rooftop solar potential, geographic information systems (GIS), deep learning, sampling strategy, city scale

NONMENCLATURE

Abbreviations	
GES	Google Earth Satellite
BIPV	Building Integrated Photovoltaic
GIS	Geographic Information System

1. INTRODUCTION

With the reduction of fossil fuels and the rapid growth of the global energy demand, many countries are seeking sustainable energy development by producing and obtaining energy in a sustainable manner [1]. Solar energy is one of the most reliable renewable energy sources in power production and the installation of BIPV systems on the rooftops has been widely accepted as a sustainable solution to make full use of urban solar energy [2].

To estimate the rooftop solar potential, it is necessary to quantify the available rooftop area of buildings that can receive solar radiation. The massive images of GES and the image semantic segmentation method based on deep learning provide a new opportunity for city scale extraction of rooftop information. The extraction results can further support the estimation of city-scale solar potential [3].

The main goal of this study is to build a specific and generalizable framework to extract building rooftops, which provides support for the large-scale assessment of solar potential of urban building rooftops. In addition, a sample acquisition strategy combining with prior knowledge is formulated to reduce the labor cost when generating the dataset for training the rooftop extraction model. By applying this model, a case study in Nanjing, China, is implemented to illustrate the extraction of rooftops with the proposed framework, and the extracted rooftop area is then used to assess the rooftop solar potential. The spatial distribution map of solar potential was further drawn to provide reference for urban solar photovoltaic deployment and urban energy policy-making.

Selection and peer-review under responsibility of the scientific committee of CUE2020

2. METHODOLOGY AND RESEARCH FRAMEWORK

2.1 Overall research framework

In this study, the solar potential of urban rooftops was estimated through four main steps. Including acquisition of training samples based on prior knowledge, optimization and preprocessing of the training sample, and rooftop extraction under deep learning method. The rooftop extraction result can be further used in rooftop solar potential estimation. The overall work framework are as follows in Figure 1.

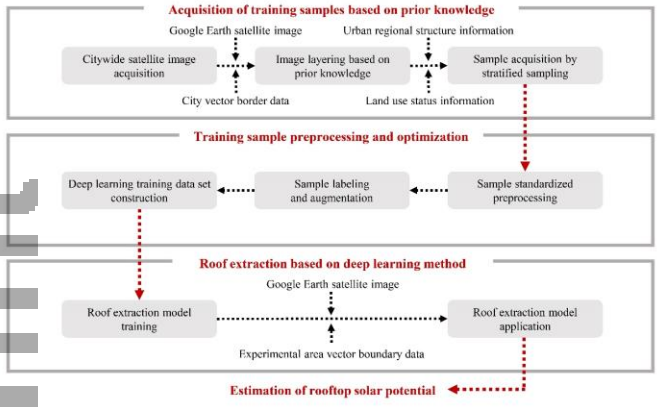

Fig 1 Research flow chart.

In the training sample acquisition part, a sampling strategy was formulated combined with prior knowledge about the city's regional structure and landuse status. In the training sample optimization and preprocessing part, the collected samples were standardized and data augmentation was performed to construct a training data set suitable for deep learning. In the rooftop extraction part, the training data set was input into the deep learning network and a model that can realize the extraction of rooftop in GES images could be further obtained. In the application of the rooftop extraction model, based on the obtained building rooftop data, combined with the clear sky radiation data and considering the impact of the actual weather conditions, we can estimate the solar potential of the rooftop in the experimental area.

2.2 Acquisition of training samples based on prior knowledge

2.2.1 Citywide GES image acquisition

This study used the publicly available GES image as the data source. Our study area was implemented in Nanjing, China, which includes 11 districts. According to the boundary of Nanjing, GES images within the whole city were downloaded via python scripts based on the open map service application program interface (Google Earth API) provided by Google. The image resolution of the downloaded GES images is about 0.25 meters/pixel. Under this resolution, the details of the building can be displayed clearly.

2.2.2 Training sample acquisition based on prior knowledge

For deep learning, the model performance improves logarithmically as the magnitude of the training data increases [4]. However, the data set should be organized with some prior knowledge instead of being increased arbitrarily. The model performance can thereby be maximized under the same sample size. From the perspective of data acquisition, the distribution and number of samples were determined in combination with urban construction in Nanjing.

The rapid urbanization of China has led to different architectural characteristics between rural and urban residential buildings [5]. In order to make the rooftop extraction model more suitable for extracting different styles of rooftops in Nanjing, the urban and rural architectural samples need to be obtained as training samples in a balanced manner. In this study, the sampling area was divided into three parts, the central zone, middle zone, and outer zone, according to the urban and rural spatial layout proposed in Nanjing urban construction plan (Figure 2).

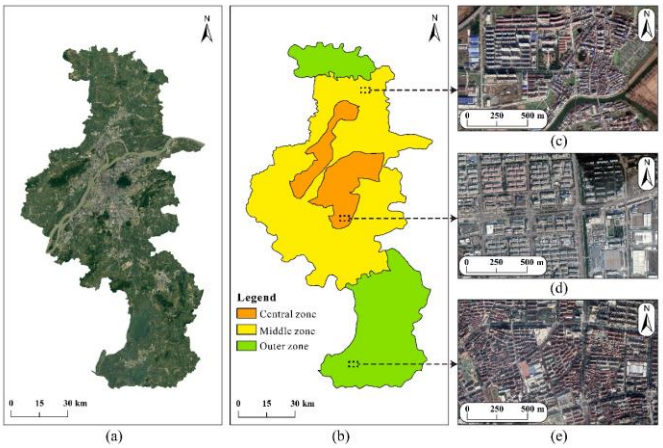

Fig 2 Sampling area layering based on the urban and rural spatial layout

The study area contains many areas such as water systems and cultivated land. But the proportion of these non-target samples is much more than our target samples (rooftop). Therefore, the samples need to be further filtered combined with the prior knowledge of urban landuse. In our study, the three sampling areas were filtered based on the landuse of Nanjing derived from the global 30-metre surface coverage data (Globeland30, www.globallandcover.com), excluding non-man-made surface areas (Figure 3).

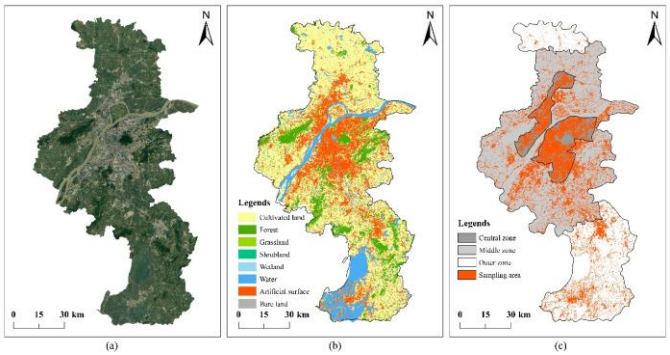

Fig 3 Sampling area filtering based on the current landuse.

By layering the sampling area according to the urban and rural spatial layout, and filtering the sampling area according to the current landuse, a sample acquisition strategy method based on prior knowledge was proposed to obtain rooftop samples with better balance and richness. Based on this strategy, a python script was written to obtain training samples from GES images throughout Nanjing.

2.3 Training sample preprocessing and optimization

2.3.1 Training sample standardized preprocessing

Despite the high resolution of the GES images of level 19, these images have been found not always satisfactory in practical work. As shown in Figure 4(a), the quality of the GES image varies with the imaging system, imaging time, and environmental factors such as the atmosphere and climate. The variation in image quality will bring a lot of interference information to the model training. Therefore, these images need to be preprocessed to improve their quality.

In this study, the brightness and clarity are the two major quality problems of GES images in Nanjing. Consequently, brightness processing and sharpness processing need to be performed. In the brightness processing step, images with abnormal brightness level were adjusted with gamma correction. In the sharpness processing step, contrast limited adaptive histogram equalization (CLAHE) was conducted to all the images. The comparison before and after GES images standardized preprocessing is shown in Figure 4(b) and Figure 4(c).

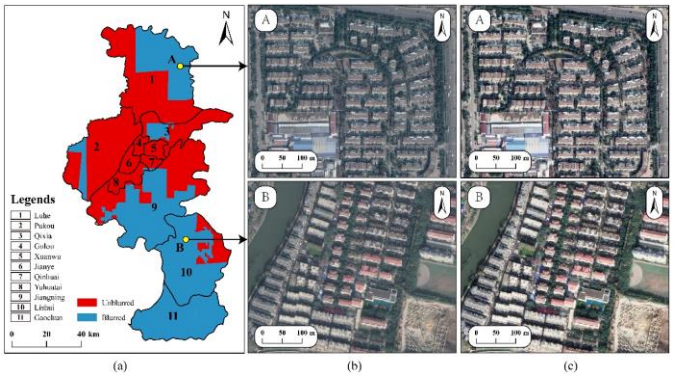

Fig 4 Comparison of GES images before and after standardized preprocessing.

2.3.2 Training sample labelling and augmentation

In the deep learning method used in this study, the image label corresponding to each training sample needs to be produced to support the model training. ArcGIS was used to mark the training sample manually. A drawing tool was used to mark the rooftops in the GES image samples one by one.

Data augmentation is implemented to obtain sufficient data for training deep networks. The GES image samples were randomly processed for data augmentation. The data augmentation methods used included image rotation, image flipping, image blurring, and noise addition (Figure 5).

Fig 5 Data augmentation.

2.4 Rooftop extraction based on the deep learning method

DeepLab v3 is the latest version of the DeepLab series of open-source image semantic segmentation models launched by the Google R&D team. Rooftops in Nanjing were extracted based on DeepLab v3 and GES images. After the GES images of Nanjing were acquired, rooftop image samples of typical areas were collected and input to DeepLab v3 for training, an ideal model suitable for Nanjing rooftop extraction was obtained. By inputting all the images of Nanjing into this model, the rooftop portions in the GES images could be identified.

2.5 Estimation and temporal analysis of rooftop solar potential

2.5.1 Estimation of the rooftop solar potential

The solar radiation data used in this study come from the Copernicus Atmosphere Monitoring Service (CAMS) (http://www.soda-pro.com/web-

services/radiation/cams-radiation-service). These data are solar radiation data at the surface level with a clear sky taken at hourly intervals, and they are publicly available free of charge. In this study, the rooftop of a building is regarded as a horizontal plane. Combined with clear sky radiation data (Wh/m^2) and cloud cover correction parameters, the total amount of solar radiation received on the rooftop of buildings is estimated.

The total solar radiation reaching the ground consists of direct radiation and diffuse radiation [6]. The formula for calculating the total radiation at the surface level is as follows [7]:

$$GHI = BHI + DHI \quad (1)$$

In the formula, *GHI* is the global horizontal irradiance, *BHI* is the direct solar radiation, and *DHI* is the diffuse horizontal irradiance.

The formula for calculating the true acceptable solar radiation in the horizontal plane is as follows [8]:

$$GHI_r = BHI \cdot M_t + DHI \cdot M_d \quad (2)$$

In the formula, GHI_r is the actual solar radiation received by the horizontal plane, *BHI* is the horizontal solar radiation under clear sky conditions, M_t is the monthly atmospheric transmittance, *DHI* is the horizontal solar radiation under clear sky conditions, and M_d is the monthly diffusion ratio.

The formulas for calculating the monthly atmospheric transmittivity (M_t) and diffuse proportion (M_d) from cloud data are as follows [8]:

$$M_t = 0.7 \cdot P_{clear} + 0.3 \cdot P_{cloudy} \quad (3)$$

$$M_d = 0.2 \cdot P_{clear} + 0.7 \cdot P_{cloudy} \quad (4)$$

In the formula, P_{clear} is the proportion of sunny days in a month, and P_{cloudy} is the proportion of cloudy days in a month. We use World Weather Online (https://www.worldweatheronline.com/) to obtain the sunny and cloudy days in each month to determine P_{clear} and P_{cloudy}.

2.5.2 Temporal analysis of the rooftop solar potential

The annual solar radiation (ASR) of all rooftop surfaces in the study area is estimated as follows:

$$ASR = \sum_{i=1}^{n_1}\left(\sum_{m=1}^{12}\left(\sum_{h=0}^{23}\left(\sum_{d=1}^{n_2}(S_i \times GHI_{rmdh})\right)\right)\right) \quad (5)$$

Here, S_i represents the area of the i^{th} rooftop, and GHI_{rmdh} represents the corrected real solar radiation between the times *h* and *h+1* in the mth month on the d^{th} day of the year. *i* represents the number of a rooftop (*i* = 1, 2, 3, ..., n_1), and n_1 represents the total number of rooftops. m represents the month (*m* = 1, 2, 3, ..., 12). h represents the time in the 24-hour system (*h* = 0, 1, 2, …, 23). The actual duration of received radiation is from sunrise to sunset on each day. d represents the day of the month (*d* = 1, 2, 3 ,...,n_2), and n_2 represents the actual number of days per month.

The input data of the model are the hourly solar radiation data, monthly atmospheric transmittance, diffusion ratio, and rooftop surface (stored in ShapeFile format). The simulation time interval is one hour. The radiation estimation results for different periods can be generated according to the research design. In this study, the total annual acceptable solar radiation and the monthly total solar radiation per hour are obtained.

3. STUDY RESULTS

3.1 Rooftop extraction results

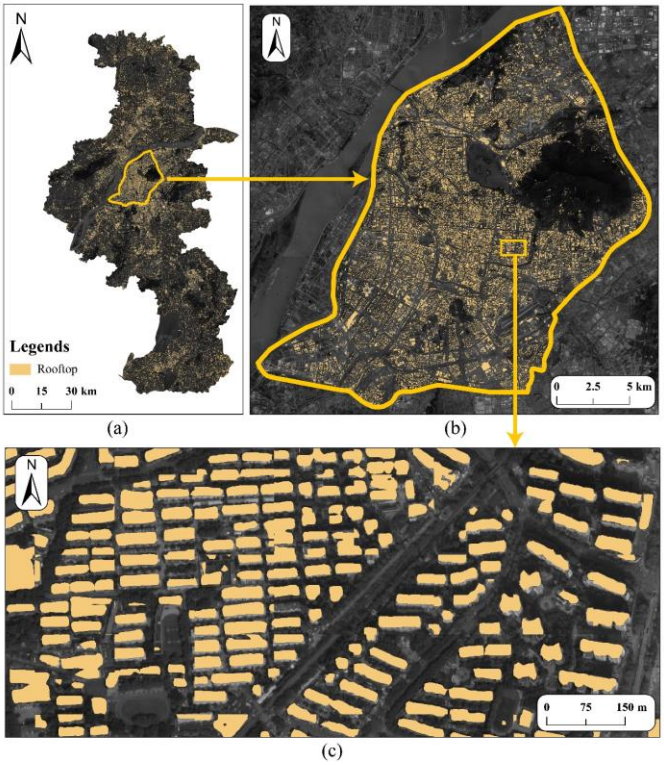

Fig 6 Results of rooftop extraction.

In Nanjing, the total rooftop area is 430.54 km^2. A more detailed rooftop extraction result is illustrated in Figure 6(b) and Figure 6(c). The performance evaluation of the rooftop extraction model based on the strategic sampling method was conducted in eleven verification areas in Nanjing. The overall model performance evaluation of both the non-strategic sampling method

and the strategic sampling method are summarized, and the results are shown in Table 1.

Tab 1 Comparison of the model performance under strategic and non-strategic sampling methods in Nanjing

Method	Accuracy	Precision	Sensitivity	F1 Score
Non-strategic sampling method	0.90	0.80	0.71	0.74
Strategic sampling method	0.93	0.84	0.79	0.82
Improvement	0.03	0.04	0.08	0.08

To further demonstrate the beneficial influence of the strategic sampling method on the study, a comparative study of sampling quantity and model accuracy is conducted. Figure 7 shows the cost-profit benefit curve under the strategic sampling method and the non-strategic sampling method. In terms of the cost input of the method promotion, the sample quantity required by the strategic sampling method is significantly smaller than that of the non-strategic sampling method when the model accuracy is equal. We can see from the red indicator line in Figure 7 that only about 12.5% of the sample amount is needed to achieve the same accuracy using strategic sampling method.

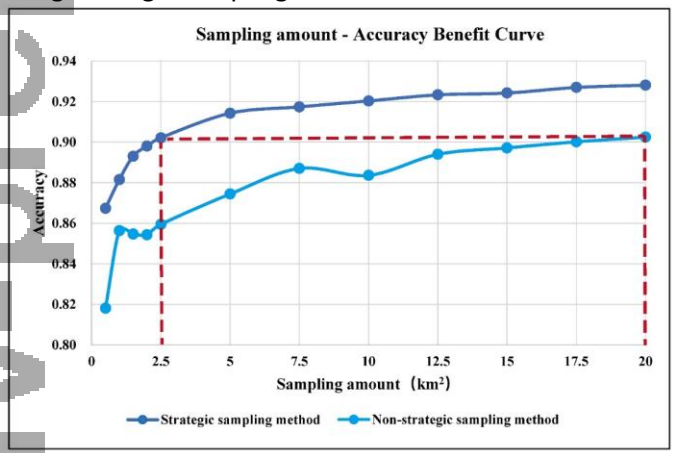

Fig 7 Cost-profit benefit curve.

3.2 *Solar potential estimation results*

Based on the rooftop extraction results for Nanjing, the solar radiation that the city's rooftops can receive was estimated. The results are displayed according to a three-level scale (Figure 8). Figure 8(a) shows the rooftop solar potential in Nanjing. Figure 8(b) shows the distribution of the estimated rooftop solar potential in downtown Nanjing. Taking a small local area as an example, the details of the estimation results are presented in Figure 8(c). It can be seen that the rooftop in Nanjing has a large solar potential according to our calculation results.

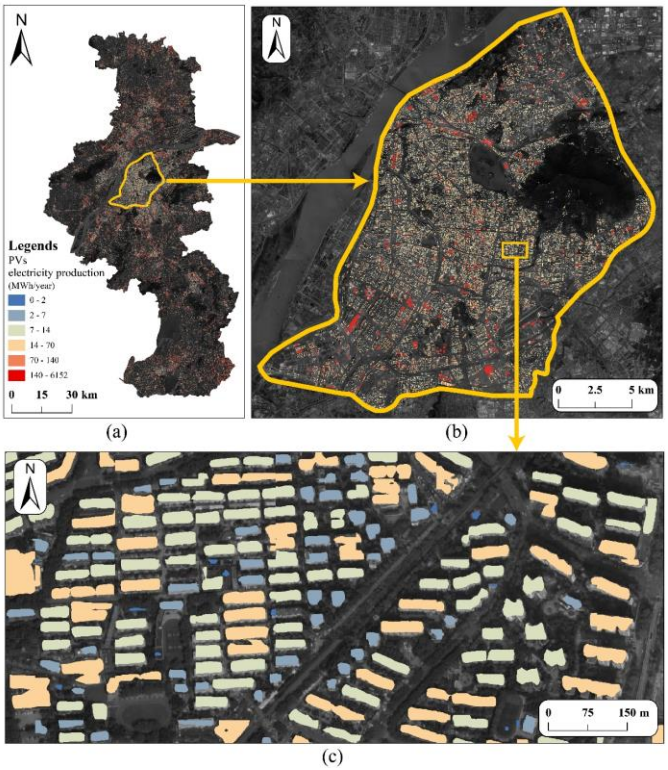

Fig 8 Solar potential on rooftops.

3.3 *Temporal analysis of the solar potential*

This study also conducted a time series analysis of the solar potential of the rooftops of buildings in Nanjing and estimated the total solar potential of the roofs of buildings in Nanjing during different periods in 2019 (Figure 9). In Figure 9, the hourly solar potential curves are divided into different colors according to the seasonal characteristics of the hourly solar potential of the rooftop: (i) Spring (green): March, April, and May; (ii) Summer (red): June, July, and August; (iii) Autumn (orange): September, October, and November; (iv) Winter (blue): December, January, and February.

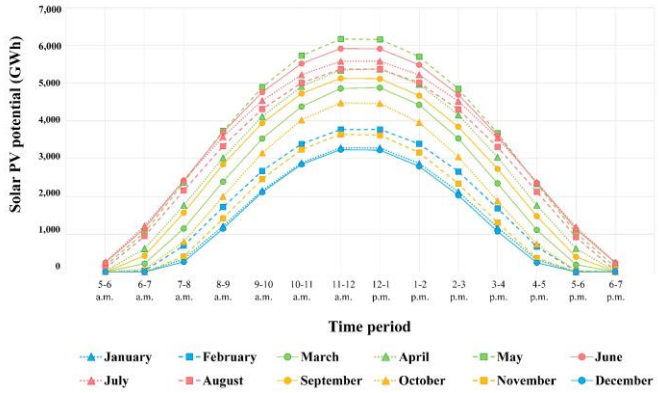

Fig 9 Rooftop solar potential in Nanjing during each month in 2019 (GWh).

It can be seen from Figure 9 that the rooftop solar potential reaches its maximum value at 11 and 12 am. This is because the elevation angle of the sun reaches its maximum value at noon. During this period of time, the level of direct radiation acceptable to the horizontal receiving surface is highest. It can also be seen that the rooftop solar potential is greatest in May and June. This is because the weather in Nanjing in May and June is mostly clear, and the sun has a higher elevation angle. In contrast, rooftop has the lowest solar potential in winter (December, January, and February). In addition to this, there are different sunrise and sunset times of each day of the year. So, some months receive zero radiation at 5-7 am and 5-8 pm.

4. CONCLUSIONS AND FUTURE STUDIES

In this study, a specific and generalizable framework is constructed to obtain the rooftop data of urban buildings, which provides support for the assessment of large-scale rooftop solar potential. Taking Nanjing as an example, the application effect of the framework is shown. Based on the sampling strategy, we first obtain a small number of rooftop samples for deep learning semantic segmentation model training. Using the trained model, the rooftop of buildings can be extracted from the massive GES images in the whole city. The accuracy of the model is 93%. Based on the rooftop data, we further calculated the solar potential of the rooftops as an application case, and obtained that the annual solar potential of the building rooftops in Nanjing is huge.

The framework developed in this study can complete the extraction of urban building rooftop without relying on 3D model, which has high flexibility and can provide support for the rapid promotion of building roof solar potential assessment in the world. In recent years, the image semantic segmentation technology under the support of deep learning has been developing, which provides a strong support for the refinement of image entity segmentation. In the future, better performance semantic segmentation network can be used to further improve the accuracy of roof extraction model. In order to simplify the estimation, the roof is assumed to be plane in the estimation of solar potential. In the future, the influence of roof structure and available area on the estimation of photovoltaic potential can be further considered. In addition, the economic cost of deploying bvap (building attached PV) system is not considered in this study. Future work needs to evaluate the economic feasibility by comparing the cost of deploying the BIPV system with the potential economic benefits of rooftop solar PV.

REFERENCE

[1] Gautam BR, Li F, Ru G. Assessment of urban roof top solar photovoltaic potential to solve power shortage problem in Nepal. Energy and Buildings 2015; 86:735-44.

[2] Jo JH, Otanicar TP. A hierarchical methodology for the mesoscale assessment of building integrated roof solar energy systems. Renewable Energy 2011; 36:2992-3000.

[3] Qi F, Wang Y. A new calculation method for shape coefficient of residential building using Google Earth. Energy and Buildings 2014; 76:72-80.

[4] Sun C, Shrivastava A, Singh S, Gupta A. Revisiting unreasonable effectiveness of data in deep learning era. IEEE International Conference on Computer Vision (ICCV) 2017

[5] Xiong Y, Liu J, Kim J. Understanding differences in thermal comfort between urban and rural residents in hot summer and cold winter climate. Building and Environment 2019; 165.

[6] El Mghouchi Y, El Bouardi A, Choulli Z, Ajzoul T. New model to estimate and evaluate the solar radiation. International Journal of Sustainable Built Environment 2014; 3:225-34.

[7] Yoshida S, Ueno S, Kataoka N, Takakura H, Minemoto T. Estimation of global tilted irradiance and output energy using meteorological data and performance of photovoltaic modules. Solar Energy 2013; 93:90-9.

[8] Huang S, Rich PM, Crabtree RL, Potter CS, Fu P. Modeling Monthly Near-Surface Air Temperature from Solar Radiation and Lapse Rate: Application over Complex Terrain in Yellowstone National Park. Physical Geography 2013; 29:158-78.